Dynamics of organic matter in the Seine Estuary (France): Bulk and structural approaches

Alexandre Thibault, Sylvie Derenne, Edith Parlanti, Christelle Anquetil, Mahaut Sourzac, Hélène Budzinski, Laura Fuster, Anniet M. Laverman, Céline Roose-Amsaleg, Eric Viollier, et al.

Dynamics of organic matter in the Seine Estuary (France) Bulk and structural approaches

Alexandre Thibault, Sylvie Derenne, Edith Parlanti, Christelle Anquetil, Mahaut Sourzac, H. Budzinski, Laura Fuster, Anniet M. Laverman, Céline Roose-Amsaleg, Eric Viollier, et al.

Dynamics of organic matter in the Seine Estuary (France): bulk and structural approaches

Alexandre Thibault [1], Sylvie Derenne [1], Edith Parlanti [2], Christelle Anquetil [1], Mahaut Sourzac [2], Hélène Budzinski [2], Laura Fuster [2], Anniet Laverman [3], Céline Roose-Amsaleg [3], Eric Viollier [4], Arnaud Huguet [1 *]

[1] Sorbonne Université, CNRS, EPHE, PSL, UMR METIS, Paris F-75005, France

[2] Univ. Bordeaux, CNRS, UMR EPOC, Talence F-33405, France

[3] Université de Rennes, CNRS, UMR ECOBIO, Rennes F-35042, France

[4] Institut de Physique du Globe de Paris, Sorbonne Paris Cité, Univ. Paris Diderot, CNRS, Paris F-75005, France

Abstract:

Estuaries are important ecosystems from environmental and economical point of views and are the place of numerous transformations of organic matter (OM) during the transfer from land to the ocean. The dynamics of OM in estuarine systems is complex and was only rarely investigated at the structural or molecular level, even though OM transformation in the estuarine aquatic and sediment compartments involves processes taking place at this level. The aim of this study was to constrain the sources and fate of the OM in the Seine Estuary, one of the largest estuaries in France. The spatiotemporal dynamics of the OM along the estuary was investigated by comparing the bulk (elemental and isotopic composition) and structural (solid state ^{13}C nuclear magnetic resonance) features of the different pools of OM – dissolved OM (DOM), particulate OM (POM) and sediment

* Corresponding author. Tel: + 33-144-275-172; fax: +33-144-275-150.

E-mail address: arnaud.huguet@sorbonne-universite.fr (A. Huguet).

OM collected during five sampling campaigns. Reverse osmosis coupled with electrodialysis (RO/ED) was used to concentrate and isolate DOM, yielding an average organic carbon recovery of 59 % (± 15 %). RO/ED had a limited effect on DOM properties, DOM showing more than 75% of similarity with initial estuarine samples based on 3D fluorescence measurements. Bulk and structural analyses of DOM, POM and sedimentary OM showed that OM is mainly of aquatic origin in the Seine Estuary, regardless the OM pool. Nevertheless, significant differences in chemical composition between the three OM pools were observed: higher C/N ratios, carbohydrate, lipid and protein content as well as lower char and lignin contents in DOM than in the other two compartments. Spatial variations of OM properties, for POM and to a lesser extent DOM, were observed along the Seine Estuary based on $\delta^{13}C$ and $\Delta^{14}C$ analyses and ^{13}C NMR-derived protein and lipid contents, showing the transition from a riverine to a marine-dominated system. In the mixing zone of the estuary, the $\Delta^{14}C$ composition of the sediment OM was related to the tidal strength, with strong tides leading to the resuspension of recent sediment OM and weak tides allowing the deposition of recent aquatic OM. Altogether, the combination of bulk and structural techniques showed that the Seine Estuary OM quality is mainly related to the compartment (DOM/POM/sediment) and to a lesser extent to the sampling zone (upstream/maximum turbidity zone/downstream). The approach proposed for the characterization of the Seine Estuary OM could be applied to other estuaries, allowing a better understanding of the complex OM dynamics in such ecosystems.

Keywords: Estuary, Organic matter, Characterization, Dynamics

1. Introduction

Estuaries are transitional zones between oceans and continents, with specific physico-chemical, biological and hydrological properties due to mixing of fresh and marine waters. These key ecosystems are characterized by unique and dynamic biodiversity and productivity. They are also the place of numerous economical activities (industry, harbors) and are under high anthropogenic pressure.

Each estuary is unique and has its own functioning, driven by specific and complex processes, difficult to integrate into global models (Herrmann et al., 2015). They especially transfer material from the

continent to the oceans, including nutrients and organic matter (OM) but they also play an important role on the CO_2 fluxes to the atmosphere (Canuel and Hardison, 2016). OM composition is permanently changing, following the variations of environmental parameters, such as salinity, light penetration, tidal range and is also dependent on its residence time in the estuary (Middelburg and Herman, 2007). Estuaries are highly reactive zones for the OM and are the place of numerous transformations and mixing of continental and marine OM (Bauer et al., 2013), which are not yet well understood. In estuaries, OM can originate from rivers, coastal ocean or be produced within the estuary itself. It can be derived from aquatic organisms or terrigenous sources. Each of these sources has a different composition, and thus a different behavior in aquatic systems.

Three OM compartments can be distinguished in these environments. In the water column, dissolved organic matter (DOM) and particulate organic matter (POM) are commonly separated by filtration, and sediment OM represents the third compartment. The different compartments interact with one another; for instance, the degradation of fresh POM can produce DOM, or the sorption of DOM on suspended solid material yields POM (Keil et al., 1997). Resuspension of sediment OM can also lead to POM and indirectly to DOM formation, but DOM and POM can also settle to form sediment OM (He et al., 2016).

The characterization of estuarine DOM is especially challenging, due to its intrinsic heterogeneity and low concentration (mean value of 4 mg/L ; Bauer and Bianchi, 2011 and references within) which decreases toward the ocean with concomitant increasing salinity (Mopper et al., 2007). DOM isolation is thus a prerequisite for molecular characterization, and it can be achieved through several techniques. The fastest method is solid phase extraction (SPE) using a combination of XAD-8 (styrene-divinyl benzene resin) and XAD-4 (acrylic ester resin; Aiken et al., 1992) or of the more recent prefabricated cartridges (mostly C18 and PPL; Dittmar et al., 2008). Whatever the used phase, acidification of the samples is required, altering the DOM chemical structure. Tangential-flow ultrafiltration (UF) has also been developed to isolate high molecular weight DOM (Benner et al., 1997). Low molecular weight compounds (<1 nm) are lost with salts, implying that UF-DOM is not representative of the initial DOM and has been shown to be enriched in carbohydrates (Helms et al., 2015). When applied to estuarine environments, the two aforementioned methods are associated with large variations in OM

recovery, commonly decreasing towards the ocean likely due to salinity increase (Louchouarn et al., 2000).

More recently, reverse osmosis coupled with electrodialysis (RO/ED), initially developed for freshwater DOM isolation (Serkiz and Perdue, 1990), was adapted to that of marine DOM (Koprivnjak et al., 2006; Vetter et al., 2007; Gurtler et al., 2008; Koprivnjak et al., 2009). RO removes water molecules, leading to the concentration of both DOM and salts. The ED step further removes salts from estuarine and marine samples. This method does not require any pretreatment of the sample and shows high recovery rates of marine DOM (70-75%; Green et al., 2014). It has been shown that RO/ED has a limited impact on DOM properties on UV spectroscopy, 3D fluorescence and elemental analyses (Helms et al., 2015, 2013; Koprivnjak et al., 2009). As far as we know, this method has not yet been applied to estuarine environments. The effect of the RO/ED isolation of estuarine DOM was assessed in the present study using UV-visible and 3D fluorescence spectroscopy techniques.

Due to the aforementioned limitations (low concentration of DOM and high concentration of salts), only a few studies were interested in the dynamics of DOM in estuarine systems at the structural or molecular level (Abdulla et al., 2010a, 2010b; Cao et al., 2018, 2016; Guo et al., 2009; Seidel et al., 2015; van Heemst et al., 2000).In most of them, the OM is characterized at a bulk level, with elemental and isotopic techniques (Cloern et al., 2002; Guo and Santschi, 1997; Raymond and Bauer, 2001; Thornton and McManus, 1994; Wang et al., 2016). Nevertheless, OM transformation in the estuarine aquatic and sediment compartments involves processes taking place at the molecular level. Additionally, simultaneous characterization of estuarine DOM, POM and sediment OM was only rarely carried out despite the constant interactions and exchanges between these three OM pools.

The aim of this study was to concomitantly constrain the sources and fate of DOM, POM and sediment OM in the Seine Estuary (NW France). Elemental, isotopic and chemical structure analyses were combined to (i) compare the characteristics and sources of OM in the different pools (DOM, POM and sediment OM) and (ii) investigate the spatial and temporal variability of OM along the Seine Estuary.

2. Materials and methods

2.1 Study site and sampling campaigns

The Seine River (France, Fig. 1) flows through Paris area (12 million inhabitants), highly impacting the quality of the water down to the estuary. The Seine Estuary is the third largest estuary in France after the Gironde and Loire along the French Atlantic coast. Its watershed represents 12% of the France area (78 600 km^2) in which 30% of the French population, 40% of the industry and 25% of the agriculture are concentrated. This 170 km macrotidal estuary extends from a dam located at Poses (KP 202; KP – kilometric point – is defined as the distance in km from the city of Paris) to the Seine Bay. The river flow ranges from 140 to 1500 m^3/s, with an average of 430 m^3/s, the maximum and minimum flows being generally observed between January and March and between August and October, respectively. The input of water from the tributaries in the estuary is usually low (12% of the total Seine flow), but during drought events, it can reach 30% of the Seine flow.

The estuary is composed of 3 parts (Fig. 1): the upstream zone with freshwater (KP 202 to KP 325), the downstream zone with seawater (starting at KP 355) and, in between, the salinity gradient zone where the maximum turbidity zone (MTZ) is located, caused by the interaction of fresh and sea water. The MTZ is unique to macrotidal estuaries and is induced by density gradient, bathymetry, salinity stratification and tide asymmetry. The MTZ can be expulsed to the sea upon high river flow and low tide but, conversely, it can move toward the upstream zone when the river flow is low and the tide is high. The tidal range varies from 3 m to 7.5 m at the mouth of the estuary (Avoine et al., 1985).

The sampling strategy was designed to study the spatiotemporal variations of the OM properties. Samples were collected during 5 campaigns, in contrasted seasons with different tidal coefficients and river flows, onboard the R/V "Côtes de la Manche" (CNRS-INSU) from January 2015 to April 2016 (Supp. Table 1). Water samples were collected along the estuary, *i.e.* in the upstream (Poses, Rouen and Caudebec; KP 202, 245 and 310 respectively), MTZ (Tancarville, Fatouville; KP 336 and 346 respectively) and downstream (Honfleur, La Carosse; KP 355 and 370 respectively) zone (Fig. 1; Supp. Table 2). Concerning the MTZ zone, sampling was achieved at a stationary point during the maximum of turbidity observed during one tidal cycle. Similarly, in the downstream zone, water was collected at high tide (i.e. at the maximum of salinity). Large volumes of water (100 L) were sampled at mid-depth (between 4 to 9 m depth) with a pump (Spido Ecc Pro 300) into Nalgen 20 L tanks before immediate filtration through pyrolyzed (400°C, 24h) Whatman GF/F 0.7 µm glass fiber filters to

separate DOM and POM. In total, 16 large water samples were collected for the study of POM, and 9 for that of DOM, as DOM isolation by RO/ED is time-consuming. In addition, 8 small sediment cores (10 cm depth) were collected at the same locations as the water samples with an UWITEC corer. They were sliced every cm for subsequent OM analysis (Supp. Table 2). After filtration, water samples containing DOM were stored at 4°C before RO/ED. Filters with POM and sediment cores were stored at -20°C and then freeze dried.

2.2 Reverse osmosis and electrodialysis

Reverse osmosis (RO) was performed using a TiA pilot with a 40 L tank and equipped with a 101.6 cm length, 6.1 cm diameter and 2.8 m² active area spiral-wound RO seawater membrane (FilmTec SW30-2540, The Dow Chemical Company, Midland, MI). The membrane was stored in a $Na_2S_2O_5$ solution (3 g/L). Before sample concentration, the whole RO device was cleaned at a pressure of 5 bar through successive rinsings with lukewarm tap water, 1 M NaOH solution, HNO_3 solution (~ 2 g/L) and deionized water (Milli-Q, Millipore). At the end of this cleaning procedure, aliquots were collected to test the device cleanliness by spectrofluorometry.

Before sample concentration, the whole system was rinsed with pure water (Elix®, Millipore). Concentration of water samples by RO was carried out at 5, 10 or 15 bar depending on the salinity of the sample (higher pressure with higher salinity). The RO step was stopped when the final sample volume reached 8-10L depending on the initial sample volume.

Electrodialysis (ED) was performed with a EUR2B-10 P pilot (AQUALYZER®, Eurodia Industrie SA). The ED stack (10 cell pairs) was equipped with AMX and CMX membranes (NEOSEPTA®-Tokuyama Corp., Japan). The total membrane surface area of any type of membrane, i.e. anionic exchange membrane (AEM) and cationic exchange membrane (CEM), was 0.2 m^2. The cathode was a stainless-steel plate and the anode was platinized titanium mesh. The ED system which was used for this study was equipped with three independent reservoirs and hydraulic circuits for the diluate, concentrate and electrodes. External 20 L tanks were used for diluate and concentrate, while the electrode compartment was the 3L internal reservoir. The system was cleaned through successive rinsing steps using solutions of 4 g/L of HCl and 4 g/L of NaOH, as previously described (Huguet et

al., 2009a). The equipment was finally rinsed with pure water (Elix®, Millipore) until (i) the conductivity in the concentrate and diluate compartments was equal to that of pure water and (ii) the pilot was considered as clean based on fluorescence analyses. For sample desalting, the electrode compartment was fed with a solution of sodium chloride at 9 g/L, the concentrate compartment with a solution of sodium chloride at 10 g/L and the diluate compartment with the solution to be desalted.

RO/ED was performed until the volume of the sample decreased to 4-6 L and the conductivity below 0.5 mS/cm. For the low salinity samples (< 5), only one step of RO and one step of ED were needed to concentrate and desalt the sample, instead of 2 for more saline samples. ED experiments were carried out at a constant voltage (14.6-14.9 V). After the RO/ED process, the sample was concentrated with a rotary evaporator (35°C, 20 mbar), until reaching a final volume of 150-200 mL. An aliquot of 30 µL was collected for further analysis and the rest of the sample was stored at -20 °C before being freeze dried. Elemental and isotopic analyses, solid state ^{13}C NMR and radiocarbon analyses were all performed on DOM samples concentrated and desalted by RO/ED and then freeze-dried.

2.3 DOC analysis

Dissolved organic carbon (DOC) contents of the water samples were measured by thermal oxidation (at 680°C) with a Pt catalyzer using a Shimadzu Total Organic Carbon analyzer (TOC-V CSN). The analyzer was calibrated using a standard solution of potassium hydrogen phthalate $C_6H_4(COOK)(COOH)$ diluted to different concentrations according to the estimated DOC content of the samples. The results are the average value of DOC measurements for at least 3 sample replicates with low standard deviation (<0.1) and variation coefficient (<2%). Two certified reference materials (SUPER 05 Lake Superior water samples, ANALAB, Environment Canada) with certified DOC contents were analyzed at the beginning and the end of each analytical series.

2.4 Ultraviolet (UV)-visible and tridimensional (3D) fluorescence spectroscopy

Chromophoric DOM (CDOM) was characterized using UV-visible spectroscopy with a Jasco V-560 spectrophotometer, as detailed in Huguet et al. (2009b). Four parameters were calculated with UV spectrometry: the slope between 275 and 295 nm ($S_{275-295}$), the slope between 350 and 400 nm ($S_{350-400}$), the ratio of these two slopes (S_R) and the ratio of absorbance at 254 nm with the absorbance at 365 nm (E2/E3).

Fluorescent DOM (FDOM) was analyzed by excitation-emission matrix (EEM) fluorescence spectroscopy with a Fluorolog FL3-22 Horiba Spex Jobin-Yvon as detailed in Huguet et al. (2009b).. In order to avoid inner-filtering effect, when the maximum absorbance (250 nm in this study) was higher than 0.1, samples were diluted with ultrapure water. The UV–visible absorbance spectrum was then recorded again to control the maximum absorbance value. This method was presently used to follow the evolution of fluorescent DOM during RO/ED from a qualitative and semi-quantitative standpoint. Four main bands were observed in fluorescence spectra as previously reported (Parlanti et al., 2000; Supp. Table 3). The analysis of six water samples in triplicate showed that the analytical uncertainty for the α, α' and β bands is lower than 1.5 %, while the variation coefficient of the γ band is lower than 5 %.

2.5 Elemental and isotopic composition

Before elemental and isotopic analyses, POM and sediment samples were decarbonated. To this end, 10 mL of 3 M HCl were added to 1 g of sediment or 100 mg of POM for 1 hour with magnetic stirring at room temperature. Samples were then rinsed using 3 × 10 mL of ultrapure water (Elga) and centrifugated.Then, decarbonated samples were stored at -20°C and freeze dried. About 2 mg of DOM (isolated by RO/ED and then freeze-dried), 4 mg of POM and 12 mg of sediment were used for elemental and isotopic analyses. They were inserted in tin capsules before analyses, performed with a Thermo Fisher Scientific Delta V Advantage at the Alyses platform (IRD – Bondy - France). The carbon and nitrogen concentrations were calibrated using tyrosine ranging from 0.05 mg to 0.5 mg. The C isotopic composition is expressed using the delta notation ($\delta^{13}C$), given in per mil relative to the Vienna Pee Dee Belemnite (VPDB) standard.

2.6 Radiocarbon dating

Radiocarbon measurements were performed (i) on decarbonated POM and sediments (16 POM as well as 7 top (0-1 cm), 6 mid (5-6 cm) and 7 bottom (9-10 cm) sediments), and (ii) directly on bulk DOM (9 samples), as they do not contain carbonates. All samples were analyzed at the French national radiocarbon dating platform (ARTEMIS) with an accelerated mass spectrometer (AMS). About 1 mg of carbon was needed to perform the measurement. The ^{14}C activities are expressed in fraction of modern Carbon (f_M) and were further transformed into the $\Delta^{14}C$ notation (equation 1; McNichol and Aluwihare, 2007) where y is the year of the sampling:

$$\Delta^{14}C\ (‰) = \left(f_M \times e^{-1/8267 \times (1950-y)} - 1\right) \times 1000 \qquad (1)$$

The year of sampling was set to 2015 for all samples even though sampling spanned over 2015 and 2016, as a 1-year variation only induced a change of less than 0.2 ‰ in the $\Delta^{14}C$ values.

2.7 Solid state ^{13}C CP MAS NMR

Solid state ^{13}C cross polarization magic angle spinning nuclear magnetic resonance (CP MAS NMR) was performed on a Bruker Avance 500 at 125 MHz for ^{13}C using 4 mm diameter zircon rotors, 14 kHz spinning rate, 1 ms contact time and 1 s repetition time. Each spectrum was decomposed and integrated using Dmfit version 20150521 (Massiot et al., 2002). The scan numbers depended on the type of sample, *i.e.* 80 000 for DOM and between 80 000 and 230 000 for POM and sediment OM. All DOM and POM samples as well as sediment slices sampled at 0-1 cm and 9-10 cm depth were analyzed by ^{13}C NMR.

2.8. Molecular Mixing Model

The molecular mixing model (MMM) proposed by Baldock et al. (2004) was applied to NMR spectra from DOM, POM and sediment samples. This model decomposes the spectra into 6 groups, based on 5 types of macromolecules: carbohydrates, proteins, lignin, lipids and char, to which carbonyls had to be added. Two calibrations – one for marine samples and another one for soil samples – were developed by Baldock et al. (2004). Different standard materials were analyzed for the development of the marine calibration: cellulose for carbohydrates, phytoplankton amino acid for proteins, a 50/50

mix of gymnosperm and angiosperm wood for lignin, oleic acid for lipids, and red pine wood heated to 300°C for char. The soil and marine calibrations are very close, with only slight differences in the composition of protein (higher contribution of aliphatic C and lower contribution of carboxylic C in the soil than in the marine calibration) and lipid (higher influence of aliphatic and aromatic C, and lower influence of methoxy and O-alkyl C in the soil than in the marine calibration) standards (Baldock et al., 2004). The marine calibration, closer to the presently studied estuarine samples than the soil one, was applied to all NMR spectra.

2.9. Statistical analysis

Due to the low number of samples, only non-parametric statistical analyses were performed to avoid any bias in the interpretation. All statistical analyses were performed using R software version 3.4.3. The Spearman rank correlation (correlation coefficient ρ and *p*-value), which allows testing both linear and non-linear correlations and is less disturbed by outliers, was used. To test the difference between 2 or more groups of data, the Kruskal and Wallis test coupled with Dunn post-hoc test (R packages FSA and rcompanion) was applied. The groups were then classified using a combination of letter (e.g. "a", "b", "ab") with a script. The threshold between the groups was fixed at a *p*-value of 0.1.

Principal Component Analyses (PCA) were performed with FactoMineR and factoextra R package on reduced and centered data.

3. Results

3.1 Isolation of the DOM

Recovery yield of RO/ED based on DOC measurements ranged from 26 % to 87 %, with a mean yield of 59%. Highest yields were obtained for low salinity samples (Poses, Rouen, Caudebec and Tancarville) and the lowest for the marine sample (La Carosse; Table 1). The DOM quality was compared before and after RO/ED isolation using UV-vis and EEM spectroscopy. For most samples, the $S_{275-295}$, $S_{350-400}$ and E2/E3 slightly increased after RO/ED processes, with a mean variation of 25%, 29% and 17% respectively, whereas no trend was observed for the S_R, with a mean variation of 19% (Supp. Table 4).

The 3D fluorescence spectra were dominated by the α' and β bands, followed by the α and γ bands (Table 5; Supp. Figure 1). Only limited variations (< 15%) in the relative abundance of the α, α' and β bands were observed after RO/ED, while the less intense γ band shows higher variability, between 15 and 45% (Supp. Table 5; Fig. 2). The highest variations in the relative abundance of the different fluorescence bands were observed for the marine sample from La Carosse.

3.2 Elemental and isotopic composition

In DOM, total organic carbon (TOC) ranged from 6.7 to 20.7% (mean 11.5%) and total nitrogen (TN) from 0.53 to 1.59% (mean 1%; Supp. Table 6). POM and sediment OM exhibited significantly lower TOC and TN values than DOM samples concentrated by RO/ED (Fig. 3). TOC ranged from 1.2 to 7.7 % (mean 3.4%) and from 0.03 to 7.1% (mean 2.6%) in POM and sediment OM, respectively. Similarly, TN ranged from 0.16 to 0.69% (mean 0.4%) and from 0.005 to 0.84% (mean 0.3%) in POM and sediment OM, respectively. The C/N atomic ratio of DOM was significantly higher than that of POM and sediment OM (Wilcoxon test, $p < 0.05$ for both), ranging from 12.1 to 15.8 in DOM, from 8.2 to 13 in POM and from 7 to 12.8 in sediment (Fig. 3).

For the three OM compartments, the $\delta^{13}C$ increased downward the estuary (Fig. 3; Supp. Table 6) without significant differences between the considered compartments, ranging from -28.5 to -23.2‰ in DOM, from -29.9 to -22.5‰ in POM and from -29.6 to -24.2‰ in sediment.

3.3 Radiocarbon composition

The proportion of radiocarbon in the different samples is expressed as $\Delta^{14}C$. Positive values of the $\Delta^{14}C$ indicate a recent sample, *i e*. post 1950, and cannot be correlated with the age, due to the morphology of the post bomb curve (Hua et al., 2013), an increase in positive $\Delta^{14}C$ values reflecting either an increase or a decrease in the age of the sample. However, samples with negative $\Delta^{14}C$ are older than 1950. The $\Delta^{14}C$ determined in the different compartments ranged from -88 to 123 ‰ (mean 27‰) for DOM, from 55 to 1015 ‰ (mean 273‰) for POM and from -110 to 123‰ (mean -20‰)

for sediment OM (Fig. 4; Supp. Table 7). Most POM samples showed higher values than DOM and sediment OM (Fig. 4).

3.4 Functional groups

^{13}C NMR spectra were recorded to identify the main functional groups in the OM samples (Fig. 5). Spectra of DOM samples were dominated by a broad peak between 0 and 60 ppm, maximizing at 23 and 40 ppm, corresponding to aliphatic C, with a shoulder at 55 ppm corresponding to methoxy C and/or C located α to amino acid groups (Fig. 5a). For POM and sediment samples, this aliphatic peak ranged between 0 and 50 ppm, maximizing at 30 ppm, with a much better resolved peak at 55 ppm (Figs. 5b and c). All samples showed an intense well-resolved peak at 72 ppm with a shoulder at 104 ppm, assigned to O-alkyl C and anomeric C from carbohydrates, respectively. A broad signal between 110 and 160 ppm encompassed aromatic and phenolic C and, finally, a well-resolved peak of carboxylic C resonated at 175 ppm. Between 200 and 210 ppm, a small signal attests to the presence of carbonyl C.

An easier comparison between the spectra can be achieved through their decomposition and integration (cf. Supporting information).

4. Discussion

4.1 Validation of the RO/ED protocol to isolate DOM

After freeze drying, DOM samples isolated by RO/ED contained between 7 and 20% OC (Supp. Fig. 1; Supp. Table 6). These values are consistent with those previously reported in literature for marine DOM isolated by RO/ED (7 to 22% of OC; Green et al., 2014; Helms et al., 2015). Although efficient in removing salts, RO/ED does not eliminate all minerals, especially $Si(OH)_4$ and $B(OH)_3$ as previously observed for marine samples (Helms et al., 2015). However, RO/ED results in a large increase in carbon concentrations, 7 to 14 times higher than in the starting samples based on DOC analyses (Table 1), thus allowing the study of DOM chemical structure. The recovery yield is variable but is generally equal or higher than 50 % (Table 1). The highest yields are associated with upstream

samples (up to 87 %). Conversely, the lowest yield (26 %) is observed for the most marine sample (La Carosse; Table 1). Due to its higher initial salt concentration, a longer ED step was necessary to reach the required conductivity (< 500 µS/cm) compared to the freshwater samples. This longer ED may have induced the loss of a larger part of the small negatively charged organic moieties (Huguet et al., 2009a). Moreover, for La Carosse, a stronger loss of sample occurred during the desalination due to membrane wear.

In addition to quantitative DOC measurements, the UV-visible properties of DOM before and after the concentration and desalting steps were compared to examine the potential qualitative changes or losses of DOM induced by RO/ED. The variations in the different parameters derived from UV-visible analyses ($S_{275-295}$, $S_{350-400}$, E2/E3 and S_R) for the Seine Estuary samples were limited, ranging between ca. 15 % and 30 % (Supp. Table 4). Such variations are consistent with those previously observed for marine DOM samples isolated by RO/ED (31% for the $S_{275-295}$, 26% for the $S_{350-400}$ and 38% for the S_R; (Helms et al., 2015, 2013). This suggests that the RO/ED process leads to limited qualitative changes of estuarine DOM.

Zsolnay (2003) has reported that, during concentration by RO, small hydrophobic molecules could aggregate, resulting in an apparent increase in the proportion of high molecular weight molecules. Such an effect should systematically lead to a decrease of the S_R after RO/ED, as this ratio is negatively correlated with the average molecular weight of DOM (Helms et al., 2008). This trend was not apparent in the present study, the S_R increasing or decreasing after RO/ED depending on the considered sample (Supp. Table 4).

3D fluorescence measurements were performed in addition to UV-visible analyses to refine qualitative DOM characterization. Limited differences in the relative abundances of the different fluorescence bands (Supp. Table 5) were observed between the initial DOM sample and the RO/ED-DOM. A decrease in the relative abundance of the γ band was generally observed after RO/ED, consistent with the loss of protein material observed by (Helms et al., 2013) when isolating marine DOM samples by RO/ED. For the low salinity samples (S < 5; Table 1) with the highest DOC yield, the fluorescence spectrum of the RO/ED-DOM was very close to that of the initial DOM (Fig. 2).

The variations in intensity between 3D fluorescence spectra (%var) were calculated as detailed in the Supporting Information. The total variation of fluorescent DOM before and after RO/ED was limited, ranging between 3.9 and 22.2% (mean 13.2 %; Supp. Table 9). The highest differences in fluorescent DOM properties induced by the RO/ED process were again observed for the marine sample from La Carosse, and were mainly related to the partial loss of protein-like material (γ band) during RO/ED as discussed above. Nevertheless, the present results show that DOM isolated by RO/ED shares at least 75% of its fluorescence properties with initial DOM, whatever the sample.

It should be noted that optical analyses only give access to a part of DOM (chromophoric DOM) and cannot ensure that the RO/ED process does not lead to substantial fractionation, as typically observed when using other isolation techniques (e.g. XAD resins or ultrafiltration). Nevertheless, UV-visible and fluorescence techniques are to date the only ones available to monitor the quality of estuarine DOM samples, due to low DOC concentration associated with rather high salt contents.

Taking this into account, both UV-visible and fluorescence analyses showed that DOM isolated by RO/ED is roughly representative of the OM initially present in the water sample, independently of the salinity, in line with previous results obtained for marine samples (Helms et al., 2015, 2013). The present data show that RO/ED allows the isolation of DOM in moderate to high yield (59 ± 15%) from estuarine/marine samples with a limited alteration of its quality. This ensures the good reliability of the bulk and structural characterization of RO/ED-isolated estuarine DOM and will allow a confident comparison of DOM, POM and sediment OM characteristics for samples from the Seine Estuary.

4.2 Characteristics and sources of OM in the different pools

Bulk (elemental and isotopic composition) and structural (^{13}C NMR) features of DOM, POM and sedimentary OM were compared in detail in the following paragraphs.

4.2.1. Comparison of DOM vs. POM and sedimentary OM

The C/N ratio, derived from elemental analysis, is classically used as a proxy for the sources – terrigenous origin, i.e. OM derived from plants/produced in soils vs. aquatic origin, i.e. in this study OM produced *in situ* in the estuary – and degradation degree of OM in aquatic environments. An

increase in the C/N ratio reflects a more degraded OM (Rice and Tenore, 1981) and/or a higher contribution of terrigenous material, as the C/N ratio of plant-derived OM is higher than 20 (Hedges et al., 1997). In contrast, algae and bacteria are enriched in N (Talbot and Johannessen, 1992), leading to C/N ratios below 10 (Meyers, 1994).

The overall low C/N ratios of DOM, POM and sedimentary OM in the Seine Estuary (< 16; Fig. 3) suggest that OM is mostly derived from aquatic sources. Among the different pools, highest C/N ratios were observed in DOM (12-16) compared to POM and sediment OM (<12, Fig. 3). This could be explained by (i) a preferential enrichment of DOM in terrigenous material and/or (ii) increased contributions of OM with a degraded signature in the dissolved pools than in the particulate and sedimentary ones.

The first hypothesis is unlikely, as ^{13}C NMR spectroscopy revealed higher terrigenous inputs in POM and sediment OM than in DOM. POM and sediment OM were indeed enriched in aromatic, phenolic and methoxy C (Fig. 5), *i.e.* in lignin moieties compared to DOM and is further confirmed by the molecular mixing model (Baldock et al., 2004; cf. section 2.8.) (Supp. Fig. 2; Supp. Table 10). Considering proteins as a proxy for aquatic OM and lignin for terrigenous OM, the protein to lignin ratio (P/L) derived from the molecular mixing model also suggests that the relative proportion of aquatic material is the highest in DOM (Fig. 6). Therefore, the difference in C/N ratio between the three OM pools should likely reflect a higher degradation stage of DOM compared to POM and sediment OM.

This is further supported by the higher carboxylic C content shown by NMR in DOM, in agreement with the oxidative degradation of OM (Kögel-Knabner, 1997). The lower degradation of labile moieties (e.g. proteins or carbohydrates) in POM than in DOM could be due to the protection of these moieties onto solid phase, thus allowing a better preservation of the labile organic matter (Keil et al., 1994). As observed in the Seine Estuary, the particulate pool of Chesapeake Bay (Loh et al., 2006) and Galveston Bay (Guo and Santschi, 1997) was suggested to have a lower degree of recycling than the dissolved pool. In addition to estuaries, higher C/N ratio in DOM than POM and sediment OM was also reported in marine environments (North Pacific and Southern Oceans; Loh and Bauer, 2000) and may similarly be explained by the more rapid decomposition of DOM than in the other two OM pools.

The difference in C/N ratio between DOM and POM has also been observed for ultrafiltered DOM (UDOM, 1-100 nm) and POM (UPOM, 0.1-60 µm) from North Pacific, suggesting that the higher C/N value of DOM may be associated with molecules smaller than 100 nm (Sannigrahi et al., 2005).

4.2.2 Comparison of POM vs sedimentary OM

Although no major difference could be evidenced between POM and sediment OM from elemental analysis, and only limited difference from ^{13}C NMR, these two compartments are discriminated by ^{14}C age. All POM samples are indeed recent (*i. e.* post 1950), whereas the age of sediment OM samples encompasses post and ante 1950 dates (Fig. 4). Several concomitant processes can be put forward to account for this difference, as partly hypothesized in the deep ocean (Wang et al., 1996): (i) rapid decomposition of aquatic, labile organic matter in the water column; (ii) preferential deposition and incorporation of "older" terrigenous OM in the sediment; (iii) bioturbation and sediment resuspension, diluting the "recent" $\Delta^{14}C$-enriched signal of surficial sediment with "older" carbon depleted in ^{14}C from deeper sediment. The first and second hypotheses are supported by the higher values of the P/L ratio in POM than in sediment, implying that the proportion of labile aquatic vs. refractory terrigenous OM is higher in the particulate pool than in sediment. Conversely, Seidel et al. (2015) have suggested that the depletion in terrigenous OM observed in estuarine water columns could be due to its sorption onto sinking particles, enriching the sediment in terrigenous OM. The third hypothesis – sediment resuspension – should also be taken into account to explain the differences in $\Delta^{14}C$ of POM and sediment OM, as in the MTZ the $\Delta^{14}C$ of sediment OM (0-1 cm, 5-6 cm and 9-10 cm) was observed to be correlated with the hydrodynamic conditions in the Seine Estuary (Fig. 7a). It can be suggested that strong tides lead to the resuspension of fresh and young ^{14}C-enriched sediment, leaving at the surface deeper and older ^{14}C-depleted sediment OM. In contrast, low tidal flows allow the deposition of young ^{14}C-enriched, autochthonous OM at the surface of the sediment (Dyer, 1995). This interpretation is further supported by the significant decrease in the P/L ratio, and thus in the proportion of aquatic OM in MTZ sediment with increasing tidal coefficients (Fig. 7b). This bioturbation/resuspension hypothesis is also emphasized by the non-linear decrease of the $\Delta^{14}C$ in the sediment OM with depth (Supp. Table 7).

4.3. Spatial variations

4.3.1. $\delta^{13}C$ and $\Delta^{14}C$ variations

$\delta^{13}C$ is a useful tracer for OM in riverine and estuarine systems (Raymond and Bauer, 2001). As the riverine OM (terrigenous OM and freshwater phytoplankton OM) is generally depleted in ^{13}C with respect to marine OM (Cloern et al., 2002), the isotopic composition of OM is commonly used to discriminate riverine versus marine sources in estuarine and coastal environments (Canuel and Hardison, 2016). Whatever the considered OM compartment, the $\delta^{13}C$ increases downward the Seine Estuary, reflecting mixing between riverine and marine OM (Fig. 3).

The downward increase in $\delta^{13}C$ has been observed along numerous estuaries (e.g. Tay, Pearl River, Mackenzie, Eble, Ems, Rhin) for POM and sediment OM (Thornton and McManus, 1994; Middelburg and Herman, 2007; Emmerton et al., 2008; Yu et al., 2010), and was also reported for DOM in the Amazon estuary (Seidel et al., 2015). Nevertheless, the detailed spatial evolution of the isotopic composition of POM was shown to be estuary-dependent based on the study of 9 European estuaries of the Atlantic Coast (Middelburg and Herman, 2007). The variation of the $\delta^{13}C$ of POM in the Seine Estuary (Supp. Figure 3a) exhibits strong similarities with the Rhine Estuary: a high variation of $\delta^{13}C$ (from -30 to -26 ‰) for salinity < 1, constant $\delta^{13}C$ (ca. -26 ‰) for salinity between 1 and 20, and an increase in $\delta^{13}C$ (reaching up to -20 ‰) downstream. These similar trends likely reflect the close properties of the Rhine and Seine estuaries, with high tides, low suspended particulate matter contents and low residence times of water due to construction works and landscape (Middelburg and Herman, 2007).

The interpretation of the $\delta^{13}C$ values of OM in estuaries may be hampered by the complexity of these ecosystems and the diversity of the OM sources. Therefore, simultaneous investigation of $\Delta^{14}C$ and $\delta^{13}C$ can provide further insights into estuarine carbon cycling (Canuel and Hardison, 2016). Detailed investigation of $\Delta^{14}C$ (as well as $\delta^{13}C$) in the dissolved organic pool of estuaries was rarely achieved, and most results were obtained for North American estuaries (Bauer and Bianchi, 2011). In riverine and estuarine ecosystems, DOM was generally observed to be ^{14}C-enriched compared to POM. This was suggested to be due to a predominant contribution from recently produced ^{14}C-enriched soil and litterfall OM in the dissolved pool, in contrast with POM mainly derived from materials with long

residence time in the river or watershed (Bianchi and Bauer, 2011 and references therein). In contrast, in oceanic and coastal settings, the average age of POM, mainly derived from contemporary phytoplankton, is generally younger than co-occurring DOM due to the preferential removal of ^{14}C-enriched young material and preferential preservation of older ^{14}C-depleted DOM along estuaries (Raymond and Bauer, 2001).

Specific trends were observed in the Seine Estuary. In contrast with most of the systems, in the riverine and brackish part (except at Fatouville July 2015) of the Seine Estuary, no significant difference could be evidenced between DOM and POM, both being of recent age (Supp. Table 7). This is likely due to the fact that these two OM pools are predominantly of aquatic origin all along the estuary (cf. section 4.2.1) and share the same contemporary carbon sources. Then, in the marine part of the estuary (Fatouville, Honfleur and La Carosse; Supp. Table 7), DOM is depleted in ^{14}C compared to DOM and POM samples collected upstream, which reflects the transition from riverine-dominated to marine-dominated area of the estuary.

Similar to $\delta^{13}C$, $\Delta^{14}C$ analyses revealed changes in DOM characteristics along the Seine Estuary. A significant decrease in $\Delta^{14}C$-DOM from upstream (between 33 ‰ and 122.9 ‰ in Poses and Caudebec) to downstream (-20.8 ‰ and -87.9 ‰ in Honfleur and La Carosse, respectively; Supp. Figure 3b. and Supp. Table 7) was observed. A decreasing trend of DOM $\Delta^{14}C$ downward estuaries was already reported for other settings (e.g. Hudson River, York and Parker Estuaries in North America; Raymond and Bauer, 2001). It may be explained either by the removal of $\Delta^{14}C$-enriched upstream DOC along estuaries and/or by the input of $\Delta^{14}C$-depleted marine DOC.

4.3.2. Estimation of riverine OM contribution in the different pools using a binary mixing model

A two-end member conservative mixing model (Shultz and Calder, 1976) based on $\delta^{13}C$ of OM was applied to investigate in more detail the relative abundance of the riverine and marine OM sources along the Seine Estuary. Eq. 2, where $\delta^{13}C$ is the isotopic composition of the sample, $\delta^{13}C_m$ is the end member value of the marine OM and $\delta^{13}C_r$ is the end member value of the riverine OM, was used to calculate the fraction of riverine OM F_r:

$$F_r = \frac{\delta^{13}C - \delta^{13}C_m}{\delta^{13}C_r - \delta^{13}C_m} \quad (2)$$

The $\delta^{13}C_r$ was set to -30‰ which is the value of $\delta^{13}C$ observed in the most upstream sample (Poses). This value is consistent with those observed in other estuaries (Middelburg and Herman, 2007). As no open marine sample was analyzed in the present study, a value of -21‰ was used for the marine end member $\delta^{13}C_m$, based on $\delta^{13}C$ measurements in open marine environment (Wada et al., 1987; Yu et al., 2010).

As expected, in the upstream zone, OM is mostly derived from riverine source (F_r 0.72 to 0.99), with DOM showing the lowest F_r values (between 0.72 and 0.83) and POM the highest ones (from 0.80 to 0.99; Fig. 8). The relative abundance of riverine vs. marine OM logically decreases in the MTZ, with almost equal contributions of these two sources in the particulate and sediment pools (mean F_r values of 0.53 and 0.57, respectively) and higher riverine contribution in the dissolved compartment at the upstream limit of the MTZ (Tancarville, mean F_r of 0.8 for DOM; Fig 8). This may reflect the rapid degradation of the labile marine DOM in the MTZ, due to the high bacterial activity encountered in this zone (Garnier et al., 2008), and resulting in an increase in the proportion of riverine OM. The higher reactivity of DOM compared to POM and sedimentary OM, inferred from the C/N and P/L ratios (cf. discussion above), may explain the lower F_r observed for DOM in the MTZ zone.

At the beginning of the downstream zone (around Honfleur), OM still results from the mixing between riverine and marine OM (Fig. 8). Nevertheless, in the most downstream sample (La Carosse), OM is mainly derived from marine source, even though a slightly higher contribution of riverine OM (ca. 35 to 40%) is observed in sediment than in POM and DOM. This is likely due to the partial degradation of labile marine OM in the water column before its deposition onto sediment, consistent with the lower values of the P/L ratio in sediment than in POM and DOM (Fig. 6).

As previously discussed, the P/L ratio derived from ^{13}C NMR data is a promising tool to assess the relative abundance of terrigenous vs. aquatic OM along estuaries. This ratio was observed to be significantly positively correlated with $\delta^{13}C$ in POM ($\rho = 0.80$, $p < 0.05$; Supp. Fig. 4) indicating that the variations in $\delta^{13}C$ along the Seine Estuary are linearly related to an increase in the relative abundance of aquatic OM and/or preferential degradation of terrigenous OM and are reflected in a

change into the macromolecular composition of OM, as detected by ^{13}C NMR. In contrast, in the sediment pool, no relationship between $\delta^{13}C$ and P/L was observed (Supp. Fig. 4), implying that the molecular composition of sedimentary OM is not only related to the mixing of riverine and marine OM, but also depends on additional processes (i.e. inputs or removals of OM), such as the resuspension of the sediment into POM or the production/transformation of OM within the sediment. Nevertheless, care should be taken when interpreting the sedimentary data, as no NMR spectra could be recorded in the downstream zone due to a too low signal to noise ratio.

4.4. Combined effect of spatial and temporal variations

To disentangle the effects of spatial and temporal variations on DOM, POM and sedimentary OM characteristics, a principal component analysis (PCA) was performed with the C/N, $\delta^{13}C$, $\Delta^{14}C$, and ^{13}C NMR-derived molecular mixing model data for all OM pools (Fig. 9). The first three dimensions explain 79.2% of the variance. The first dimension is positively linked to the lignin (23.7% of the dimension) and char (22.8% of the dimension) content and negatively to protein (17.8% of the dimension), lipid (16% of the dimension) content and C/N (12.9% of the dimension). The second dimension is negatively linked to carbohydrate content (26.1% of the dimension) and positively to $\delta^{13}C$ (18.7% of the dimension), lipid content (14.2% of the dimension), $\Delta^{14}C$ (13.9% of the dimension) and protein content (12.4% of the dimension).

The PCA highlights the differences in chemical composition between DOM on the one hand and POM and sediment OM on the other hand. Indeed, a higher C/N ratio, carbohydrate, lipid and protein content as well as a lower char and lignin content was observed in DOM than in the other two compartments (Fig. 9). This is consistent with the more labile and hydrophilic nature of DOM.

The PCA also shows that bulk and structural characteristics of upstream POM are close to those of upstream/MTZ sediment OM in the estuary, implying a limited degradation of POM during the sedimentation or within the sediment. In contrast, in the MTZ and in the downstream zone, the difference between POM and sediment OM is much higher, implying that POM is transformed during the sedimentation processes or rapidly within the sediment. Despite their location at the beginning of

the downstream zone, Honfleur samples share several similarities with those from the MTZ, in contrast with the samples from La Carosse in the bay of Seine.

For POM and to a lesser extent DOM, the PCA also emphasizes the spatial variation of OM properties, as most samples are aligned following the $\delta^{13}C$ composition. This shows that within a compartment, the main driver of the OM composition is the mixing of freshwater (riverine OM) and seawater (marine OM). In contrast, no seasonal effect can be evidenced on DOM, POM and sedimentary OM composition. Altogether, the PCA shows that in the Seine Estuary OM quality mainly depends on its compartment (DOM/POM/sediment) and to a lesser extent on the sampling zone (upstream/MTZ/downstream).

5. Conclusion

The source and fate of DOM, POM and sedimentary OM in the Seine Estuary were investigated using bulk and structural analytical techniques. Such a study required beforehand the isolation of sufficient amounts of DOM, which was performed using RO/ED. The latter was shown for the first time to be an efficient method to isolate estuarine DOM, with only limited qualitative modifications of DOM properties according to spectroscopic analyses.

The coupling of elemental, isotopic and ^{13}C NMR analyses allowed a better understanding of the complex dynamics of DOM, POM and sediment OM in the Seine estuary. Whatever the compartment, OM was mostly of recent aquatic origin. Nevertheless, each OM pool had its own properties and dynamics, the sediment and POM being enriched in terrigenous material in comparison with DOM, whereas DOM is enriched in degraded aquatic material. This difference could be due to the higher affinity of labile polar moieties for water, whereas hydrophobic terrigenous OM may have higher affinity for the solid phase. The current multi-compartment study was required to disentangle the processes and transformations of OM from land to ocean, as each of these exhibits specific properties. The radiocarbon analysis allows the recognition of 2 zones within the estuary: a river-dominated zone with recent DOM and POM and a marine-dominated one with old DOM and recent POM. Moreover, the dynamics of sediment OM seems to be linked to the hydrodynamic conditions within the estuary, with its remobilization into POM during strong tide, and the deposit of aquatic-enriched OM during

weak tide. The Protein/Lignin ratio calculated from the ^{13}C NMR-based molecular mixing model especially appeared as a promising proxy to discriminate the sources of estuarine OM, in combination with classical elemental and isotopic analyses. In addition to the compartment of OM, the main factor driving the OM composition along the Seine Estuary was shown to be the mixing of fresh and marine waters. The approach proposed for the OM characterization of the Seine Estuary could be applied to other estuaries, especially European ones, which were much less investigated than those from North America.

Acknowledgments:

We acknowledge support from the GIP Seine-Aval through the funding of the MOSAIC project (2014-2017) and the Ile-de-France region (PhD scholarship to A. Thibault). ^{14}C dating was performed at the ARTEMIS platform funded by the INSU (CNRS, France). The authors warmly thank the crew of the "Côtes de la Manche" who helped during sampling, Clara Micheau for the sampling and the isolation of DOM, and M. Mendez (IRD Bondy) for elemental and isotopic analyses. Two anonymous reviewers are thanked for constructive comments.

References:

Abdulla, H.A.N., Minor, E.C., Dias, R.F., Hatcher, P.G., 2010a. Changes in the compound classes of dissolved organic matter along an estuarine transect: A study using FTIR and 13C NMR. Geochim. Cosmochim. Acta 74, 3815–3838.

Abdulla, H.A.N., Minor, E.C., Hatcher, P.G., 2010b. Using Two-Dimensional Correlations of 13C NMR and FTIR To Investigate Changes in the Chemical Composition of Dissolved Organic Matter along an Estuarine Transect. Environ. Sci. Technol. 44, 8044–8049.

Aiken, G.R., McKnight, D.M., Thorn, K.A., Thurman, E.M., 1992. Isolation of hydrophilic organic acids from water using nonionic macroporous resins. Org. Geochem. 18, 567–573.

Avoine, J., Dubrulle, L., Larsonneur, C., 1985. La dynamique sedimentaire dans les estuaires de la Baie de Seine. Consequences sur l''environnement. Presented at the La Baie de Seine. Colloque National du CNRS, 24-26 avril 1985.

Baldock, J.A., Masiello, C.A., Gélinas, Y., Hedges, J.I., 2004. Cycling and composition of organic matter in terrestrial and marine ecosystems. Mar. Chem., New Approaches in Marine Organic Biogeochemistry: A Tribute to the Life and Science of John I. Hedges 92, 39–64.

Bauer, J.E., Bianchi, T.S., 2011. Dissolved Organic Carbon Cycling and Transformation, in: Treatrise on Estuarine and Coastal Science. Academic Press.

Bauer, J.E., Cai, W.-J., Raymond, P.A., Bianchi, T.S., Hopkinson, C.S., Regnier, P.A.G., 2013. The changing carbon cycle of the coastal ocean. Nature 504, 61–70.

Benner, R., Biddanda, B., Black, B., McCarthy, M., 1997. Abundance, size distribution, and stable carbon and nitrogen isotopic compositions of marine organic matter isolated by tangential-flow ultrafiltration. Mar. Chem. 57, 243–263.

Bianchi, T.S., Bauer, J.E., 2011. Particulate Organic Carbon Cycling and Transformation, in: Treatrise on Estuarine and Coastal Science. Academic Press.

Canuel, E.A., Hardison, A.K., 2016. Sources, Ages, and Alteration of Organic Matter in Estuaries. Annu. Rev. Mar. Sci. 8, 409–434.

Cao, X., Aiken, G.R., Butler, K.D., Huntington, T.G., Balch, W.M., Mao, J., Schmidt-Rohr, K., 2018. Evidence for major input of riverine organic matter into the ocean. Org. Geochem. 116, 62–76.

Cao, X., Aiken, G.R., Spencer, R.G.M., Butler, K., Mao, J., Schmidt-Rohr, K., 2016. Novel insights from NMR spectroscopy into seasonal changes in the composition of dissolved organic matter exported to the Bering Sea by the Yukon River. Geochim. Cosmochim. Acta 181, 72–88.

Cloern, J.E., Canuel, E.A., Harris, D., 2002. Stable carbon and nitrogen isotope composition of aquatic and terrestrial plants of the San Francisco Bay estuarine system. Limnol. Oceanogr. 47, 713–729.

Coble, P.G., 1996. Characterization of marine and terrestrial DOM in seawater using excitation-emission matrix spectroscopy. Mar. Chem. 51, 325–346.

Dittmar, T., Koch, B., Hertkorn, N., Kattner, G., 2008. A simple and efficient method for the solid-phase extraction of dissolved organic matter (SPE-DOM) from seawater. Limnol. Oceanogr. Methods 6, 230–235.

Dyer, K.R., 1995. Chapter 14 Sediment Transport Processes in Estuaries, in: Perillo, G.M.E. (Ed.), Developments in Sedimentology, Geomorphology and Sedimentology of Estuaries. Elsevier, pp. 423–449.

Emmerton, C.A., Lesack, L.F.W., Vincent, W.F., 2008. Nutrient and organic matter patterns across the Mackenzie River, estuary and shelf during the seasonal recession of sea-ice. J. Mar. Syst. 74, 741–755.

Garnier, J., Billen, G., Coste, M., 1995. Seasonal succession of diatoms and Chlorophyceae in the drainage network of the Seine River: Observation and modeling. Limnol. Oceanogr. 40, 750–765.

Goldman, J., Hansell, D., R. Dennett, M., 1992. Chemical characterization of three large oceanic diatoms: Potential impact on water column chemistry. Mar. Ecol.-Prog. Ser. - MAR ECOL-PROGR SER 88, 257–270.

Green, N.W., Perdue, E.M., Aiken, G.R., Butler, K.D., Chen, H., Dittmar, T., Niggemann, J., Stubbins, A., 2014. An intercomparison of three methods for the large-scale isolation of oceanic dissolved organic matter. Mar. Chem. 161, 14–19.

Guo, L., Santschi, P.H., 1997. Isotopic and elemental characterization of colloidal organic matter from the Chesapeake Bay and Galveston Bay. Mar. Chem. 59, 1–15.

Guo, L., White, D.M., Xu, C., Santschi, P.H., 2009. Chemical and isotopic composition of high-molecular-weight dissolved organic matter from the Mississippi River plume. Mar. Chem. 114, 63-71.

Gurtler, B.K., Vetter, T.A., Perdue, E.M., Ingall, E., Koprivnjak, J.-F., Pfromm, P.H., 2008. Combining reverse osmosis and pulsed electrical current electrodialysis for improved recovery of dissolved organic matter from seawater. J. Membr. Sci. 323, 328–336.

He, W., Chen, M., Schlautman, M.A., Hur, J., 2016. Dynamic exchanges between DOM and POM pools in coastal and inland aquatic ecosystems: A review. Sci. Total Environ. 551, 415–428.

Helms, J.R., Mao, J., Chen, H., Perdue, E.M., Green, N.W., Hatcher, P.G., Mopper, K., Stubbins, A., 2015. Spectroscopic characterization of oceanic dissolved organic matter isolated by reverse osmosis coupled with electrodialysis. Mar. Chem. 177, Part 2, 278–287.

Helms, J.R., Stubbins, A., Perdue, E.M., Green, N.W., Chen, H., Mopper, K., 2013. Photochemical bleaching of oceanic dissolved organic matter and its effect on absorption spectral slope and fluorescence. Mar. Chem. 155, 81–91.

Helms, J.R., Stubbins, A., Ritchie, J.D., Minor, E.C., Kieber, D.J., Mopper, K., 2008. Absorption spectral slopes and slope ratios as indicators of molecular weight, source, and photobleaching of chromophoric dissolved organic matter. Limnol. Oceanogr. 53, 955–969.

Herrmann, M., Najjar, R.G., Kemp, W.M., Alexander, R.B., Boyer, E.W., Cai, W.-J., Griffith, P.C., Kroeger, K.D., McCallister, S.L., Smith, R.A., 2015. Net ecosystem production and organic

carbon balance of U.S. East Coast estuaries: A synthesis approach. Glob. Biogeochem. Cycles 29, 96–111.

Hua, Q., Barbetti, M., Rakowski, A.Z., 2013. Atmospheric Radiocarbon for the Period 1950–2010. Radiocarbon 55, 2059–2072.

Huguet, A., Balmann, H.R., Parlanti, E., 2009a. Fluorescence spectroscopy applied to the optimisation of a desalting step by electrodialysis for the characterisation of marine organic matter. J. Membr. Sci. 326, 186–196.

Huguet, A., Vacher, L., Relexans, S., Saubusse, S., Froidefond, J.M., Parlanti, E., 2009b. Properties of fluorescent dissolved organic matter in the Gironde Estuary. Org. Geochem. 40, 706–719.

Keil, R.G., Mayer, L.M., Quay, P.D., Richey, J.E., Hedges, J.I., 1997. Loss of organic matter from riverine particles in deltas. Geochim. Cosmochim. Acta 61, 1507–1511.

Keil, R.G., Montluçon, D.B., Prahl, F.G., Hedges, J.I., 1994. Sorptive preservation of labile organic matter in marine sediments. Nature 370, 549–552.

Kögel-Knabner, I., 1997. 13C and 15N NMR spectroscopy as a tool in soil organic matter studies. Geoderma, NMR in Soil Science 80, 243–270.

Koprivnjak, J.F., Perdue, E.M., Pfromm, P.H., 2006. Coupling reverse osmosis with electrodialysis to isolate natural organic matter from fresh waters. Water Res. 40, 3385–3392.

Koprivnjak, J.-F., Pfromm, P.H., Ingall, E., Vetter, T.A., Schmitt-Kopplin, P., Hertkorn, N., Frommberger, M., Knicker, H., Perdue, E.M., 2009. Chemical and spectroscopic characterization of marine dissolved organic matter isolated using coupled reverse osmosis–electrodialysis. Geochim. Cosmochim. Acta 73, 4215–4231.

Lesourd, S., Lesueur, P., Fisson, C., Dauvin, J.-C., 2016. Sediment evolution in the mouth of the Seine estuary (France): A long-term monitoring during the last 150years. Comptes Rendus Geosci. 348, 442–450.

Loh, A.N., Bauer, J.E., 2000. Distribution, partitioning and fluxes of dissolved and particulate organic C, N and P in the eastern North Pacific and Southern Oceans. Deep Sea Res. Part Oceanogr. Res. Pap. 47, 2287–2316.

Loh, A.N., Bauer, J.E., Canuel, E.A., 2006. Dissolved and particulate organic matter source-age characterization in the upper and lower Chesapeake Bay: A combined isotope and biochemical approach. Limnol. Oceanogr. 51, 1421–1431.

Louchouarn, P., Opsahl, S., Benner, R., 2000. Isolation and Quantification of Dissolved Lignin from Natural Waters Using Solid-Phase Extraction and GC/MS. Anal. Chem. 72, 2780–2787.

Mao, J., Cao, X., Olk, D.C., Chu, W., Schmidt-Rohr, K., 2017. Advanced solid-state NMR spectroscopy of natural organic matter. Prog. Nucl. Magn. Reson. Spectrosc. 100, 17–51.

Massiot, D., Fayon, F., Capron, M., King, I., Le Calvé, S., Alonso, B., Durand, J.-O., Bujoli, B., Gan, Z., Hoatson, G., 2002. Modelling one- and two-dimensional solid-state NMR spectra. Magn. Reson. Chem. 40, 70–76.

McNichol, A.P., Aluwihare, L.I., 2007. The power of radiocarbon in biogeochemical studies of the marine carbon cycle: insights from studies of dissolved and particulate organic carbon (DOC and POC). Chem. Rev. 107, 443–466.

Meyers, P.A., 1994. Preservation of elemental and isotopic source identification of sedimentary organic matter. Chem. Geol. 114, 289–302.

Middelburg, J.J., Herman, P.M.J., 2007. Organic matter processing in tidal estuaries. Mar. Chem. 106, 127–147.

Mopper, K., Stubbins, A., Ritchie, J.D., Bialk, H.M., Hatcher, P.G., 2007. Advanced Instrumental Approaches for Characterization of Marine Dissolved Organic Matter: Extraction Techniques, Mass Spectrometry, and Nuclear Magnetic Resonance Spectroscopy. Chem. Rev. 107, 419–442.

Parlanti, E., Wörz, K., Geoffroy, L., Lamotte, M., 2000. Dissolved organic matter fluorescence spectroscopy as a tool to estimate biological activity in a coastal zone submitted to anthropogenic inputs. Org. Geochem. 31, 1765–1781.

Raymond, P.A., Bauer, J.E., 2001. Use of 14C and 13C natural abundances for evaluating riverine, estuarine, and coastal DOC and POC sources and cycling: a review and synthesis. Org. Geochem. 32, 469–485.

Rice, D.L., Tenore, K.R., 1981. Dynamics of carbon and nitrogen during the decomposition of detritus derived from estuarine macrophytes. Estuar. Coast. Shelf Sci. 13, 681–690.

Sannigrahi, P., Ingall, E.D., Benner, R., 2005. Cycling of dissolved and particulate organic matter at station Aloha: Insights from 13C NMR spectroscopy coupled with elemental, isotopic and molecular analyses. Deep Sea Res. Part Oceanogr. Res. Pap. 52, 1429–1444.

Seidel, M., Yager, P.L., Ward, N.D., Carpenter, E.J., Gomes, H.R., Krusche, A.V., Richey, J.E., Dittmar, T., Medeiros, P.M., 2015. Molecular-level changes of dissolved organic matter along the Amazon River-to-ocean continuum. Mar. Chem. 177, Part 2, 218–231.

Serkiz, S.M., Perdue, E.M., 1990. Isolation of dissolved organic matter from the suwannee river using reverse osmosis. Water Res. 24, 911–916.

Shultz, D.J., Calder, J.A., 1976. Organic carbon 13C12C variations in estuarine sediments. Geochim. Cosmochim. Acta 40, 381–385.

Talbot, M.R., Johannessen, T., 1992. A high resolution palaeoclimatic record for the last 27,500 years in tropical West Africa from the carbon and nitrogen isotopic composition of lacustrine organic matter. Earth Planet. Sci. Lett. 110, 23–37.

Thornton, S.F., McManus, J., 1994. Application of Organic Carbon and Nitrogen Stable Isotope and C/N Ratios as Source Indicators of Organic Matter Provenance in Estuarine Systems: Evidence from the Tay Estuary, Scotland. Estuar. Coast. Shelf Sci. 38, 219–233.

van Heemst, J.D.H., Megens, L., Hatcher, P.G., de Leeuw, J.W., 2000. Nature, origin and average age of estuarine ultrafiltered dissolved organic matter as determined by molecular and carbon isotope characterization. Org. Geochem. 31, 847–857.

Vetter, T.A., Perdue, E.M., Ingall, E., Koprivnjak, J.-F., Pfromm, P.H., 2007. Combining reverse osmosis and electrodialysis for more complete recovery of dissolved organic matter from seawater. Sep. Purif. Technol. 56, 383–387.

Wada, E., Minagawa, M., Mizutani, H., Tsuji, T., Imaizumi, R., Karasawa, K., 1987. Biogeochemical studies on the transport of organic matter along the Otsuchi River watershed, Japan. Estuar. Coast. Shelf Sci. 25, 321–336.

Wang, X.-C., Druffel, E.R.M., Lee, C., 1996. Radiocarbon in organic compound classes in particulate organic matter and sediment in the deep northeast Pacific Ocean. Geophys. Res. Lett. 23, 3583–3586.

Wang, X., Xu, C., Druffel, E.M., Xue, Y., QI, Y., 2016. Two black carbon pools transported by the Changjiang and Huanghe Rivers in China. Global Biogeochem. Cycles 30, 1778-1790.

Yu, F., Zong, Y., Lloyd, J.M., Huang, G., Leng, M.J., Kendrick, C., Lamb, A.L., Yim, W.W.-S., 2010. Bulk organic δ13C and C/N as indicators for sediment sources in the Pearl River delta and estuary, southern China. Estuar. Coast. Shelf Sci. 87, 618–630.

Zsolnay, Á., 2003. Dissolved organic matter: artefacts, definitions, and functions. Geoderma, Ecological aspects of dissolved organic matter in soils 113, 187–209.

Figure captions

Figure 1. Map of the Seine Estuary with the position of the maximum turbidity zone (MTZ). The grey zones represent the urban area. Red dots are the locations of the sampling sites.

Figure 2. 3D fluorescence spectra of DOM samples from Tancarville (January 2015) before (left panel) and after (right panel) RO/ED process. Spectra are presented in the same scale with a normalized fluorescence unit (between 0 = minimal measured fluorescence, and 1 = maximal measured fluorescence).

Figure 3. $\delta^{13}C$ *vs.* C/N diagram for all samples (DOM, POM and SED OM). Circles, squares and diamonds represent DOM (isolated by RO/ED), POM and sediment OM, respectively. The color corresponds to the location of the sampling site.

Figure 4. $\Delta^{14}C$ of DOM (isolated by RO/ED), POM and sediment OM along the Seine Estuary. The dashed line represents the 0 value, data above this point are post 1950 (post bomb) and those below are ante 1950.

Figure 5. ^{13}C NMR spectra of samples collected in April 2016: (a) DOM isolated by RO/ED from Poses, (b) POM from Rouen and (c) surficial sediment (0-1 cm depth) from Rouen. Raw spectra are presented in black, deconvolution peaks in grey and the result of the deconvolution modeling is shown in red.

Figure 6. Protein/Lignin ratio inferred from the ^{13}C NMR molecular mixing model developed by Baldock et al. (2014) for DOM (isolated by RO/ED), POM and sediment OM. Letters are attributed based on the results of Dunn's test (threshold of 0.1).

Figure 7. Correlation between (a) the $\Delta^{14}C$ of sediment OM (0-1 cm, 5-6 cm and 9-10 cm) in the MTZ and (b) the Protein/Lignin ratio with the tide coefficient for 0-1 and 9-10 cm sediment OM.

Figure 8. Fraction of riverine OM (F_r) in the 3 zones of the Seine estuary (upstream, MTZ and downstream) for the 3 OM compartments (DOM, POM and sediment OM).

Figure 9. Dimension 1 (43.9% of the variance) and 2 (23.3% of the variance) of the PCA based on C/N, $\delta^{13}C$, $\Delta^{14}C$, and NMR-derived molecular mixing model data for DOM, POM and sediment OM (0-1 and 9-10 cm) collected along the Seine Estuary. Diamond symbols correspond to samples collected upstream, squares to those collected in the MTZ and circles to those collected downstream. The digits represent the different sampling campaigns.

Figure 1:

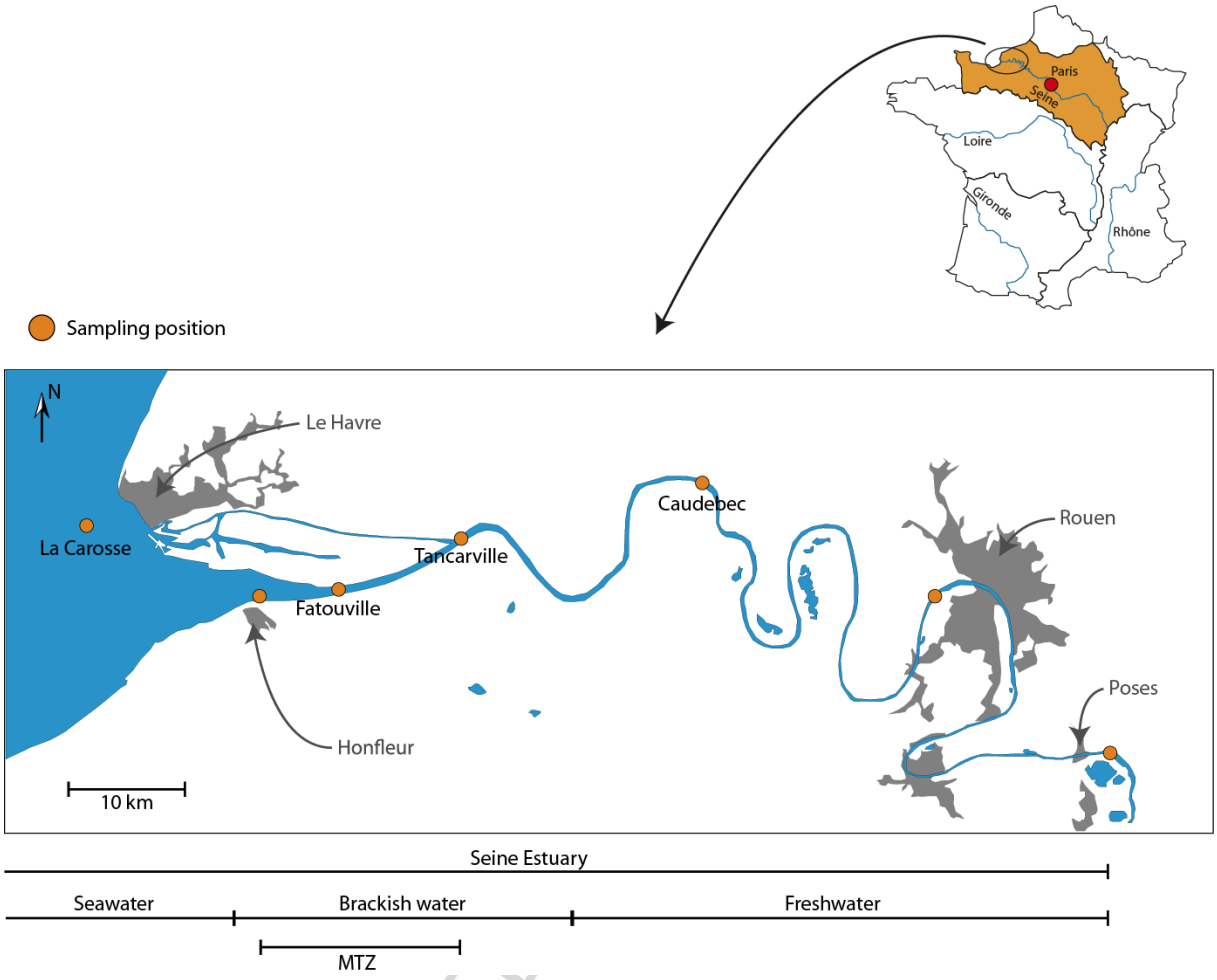

Figure 2:

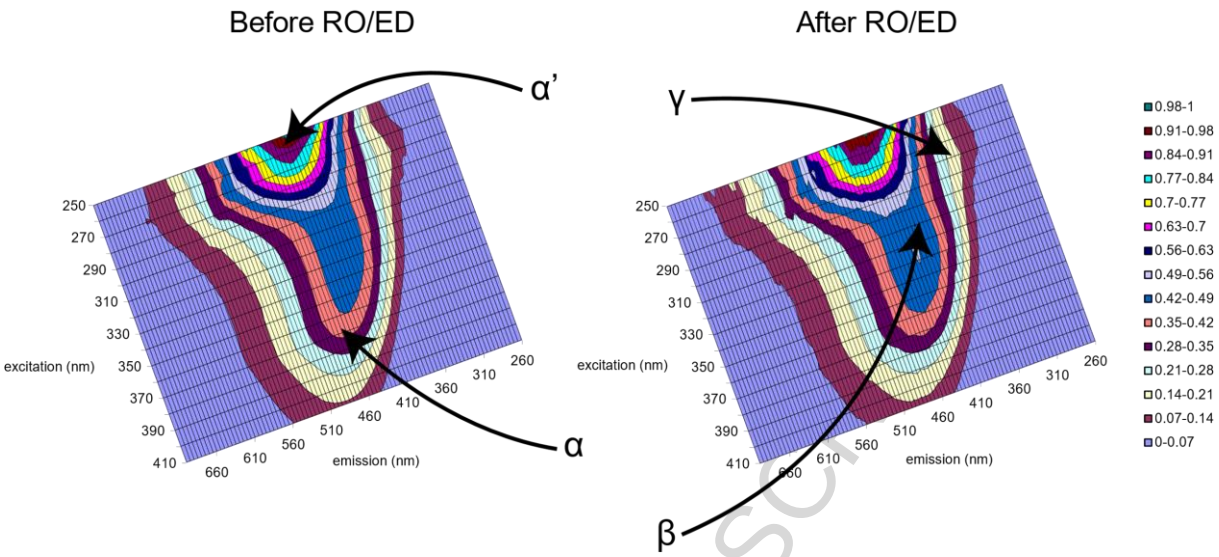

Figure 3 :

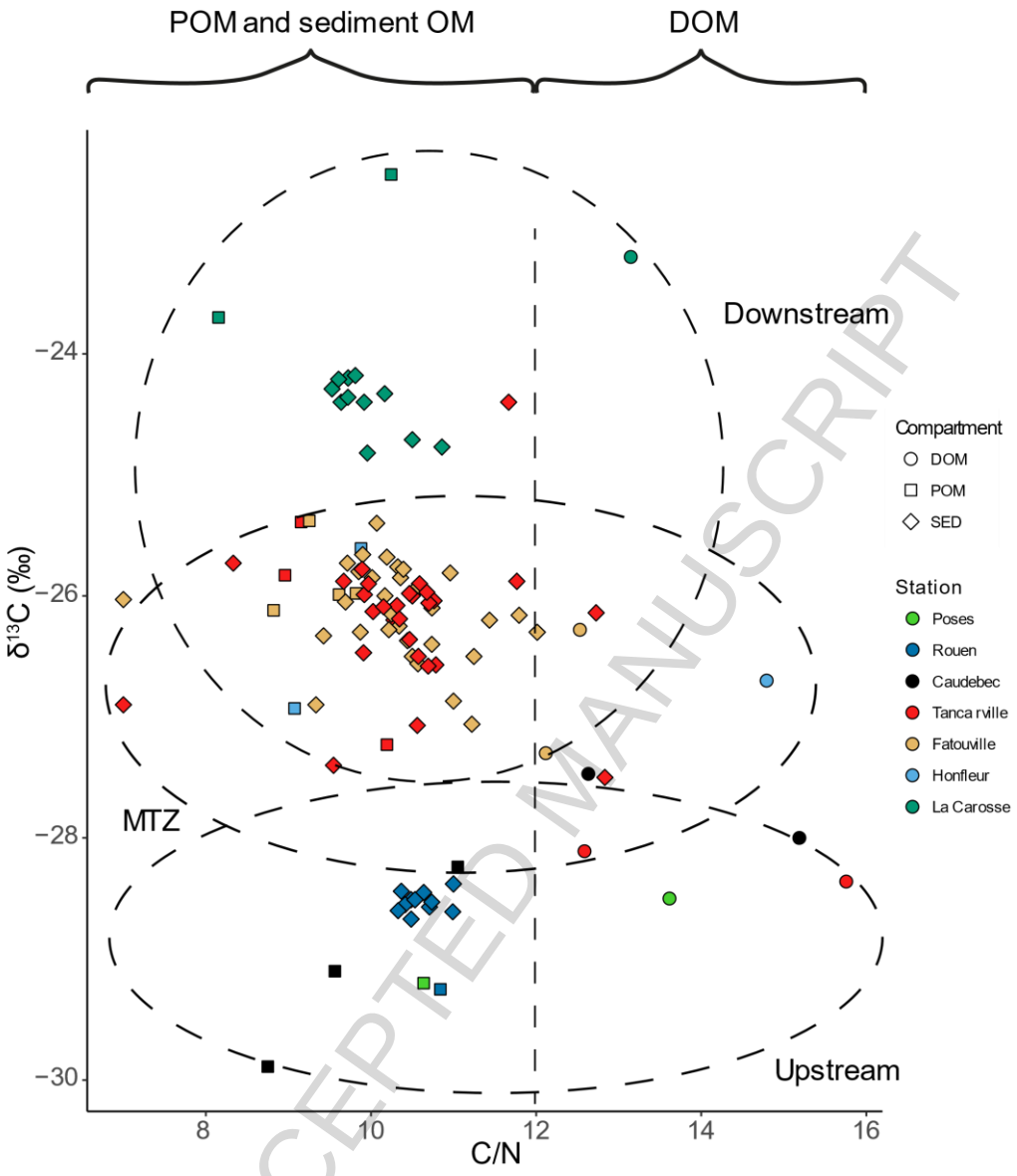

Figure 4:

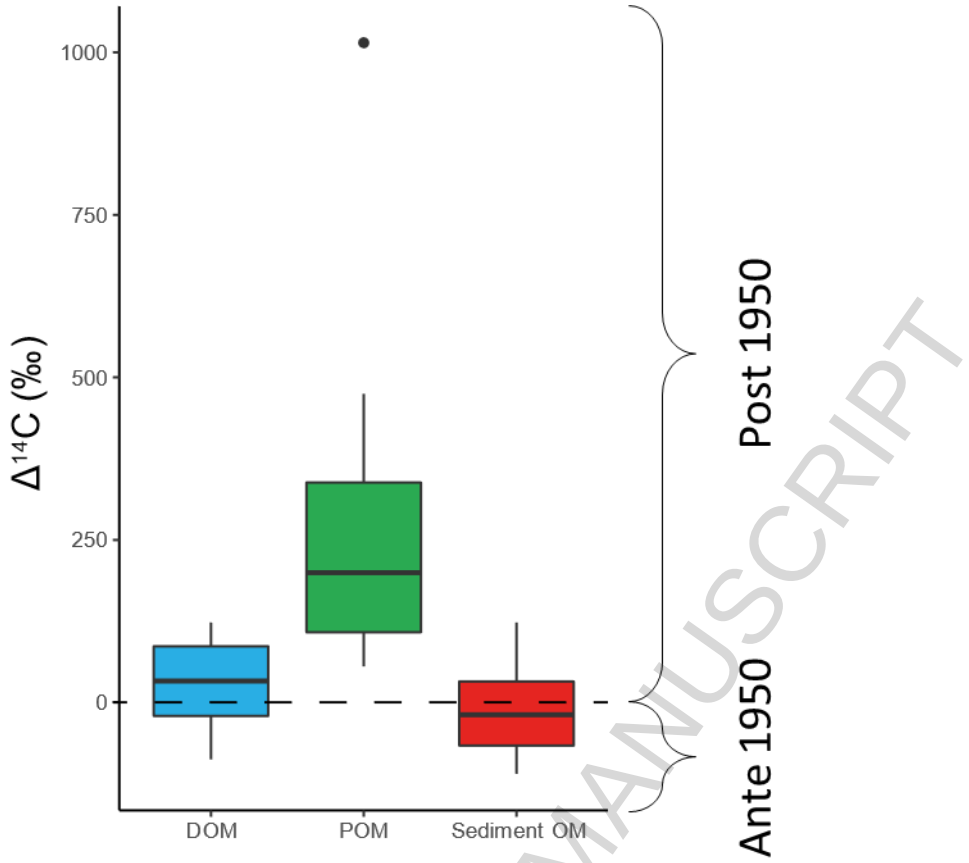

Figure 5:

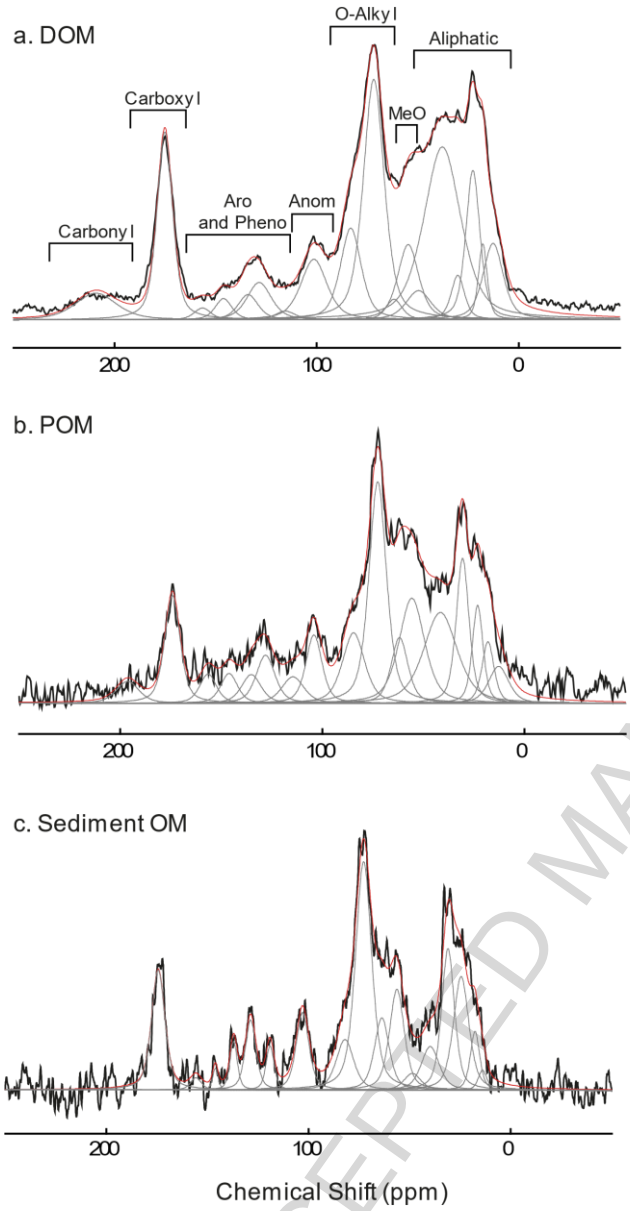

Figure 6:

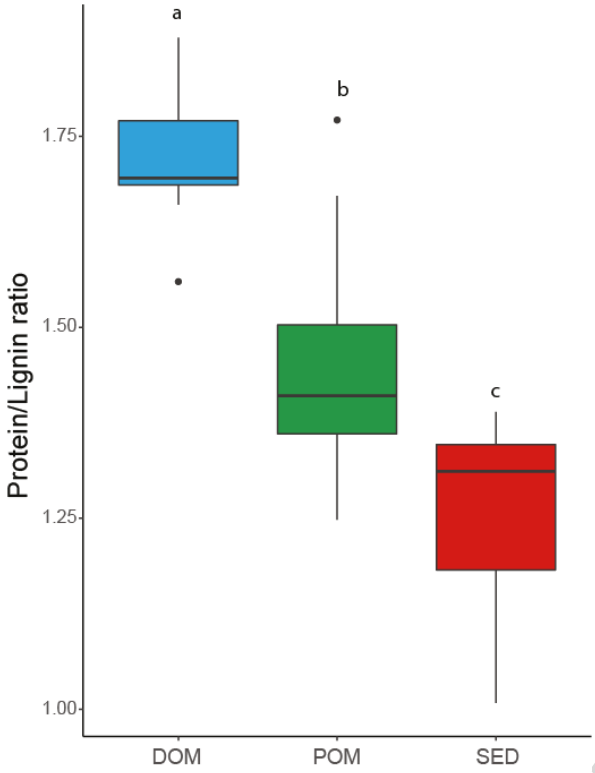

Figure 7:

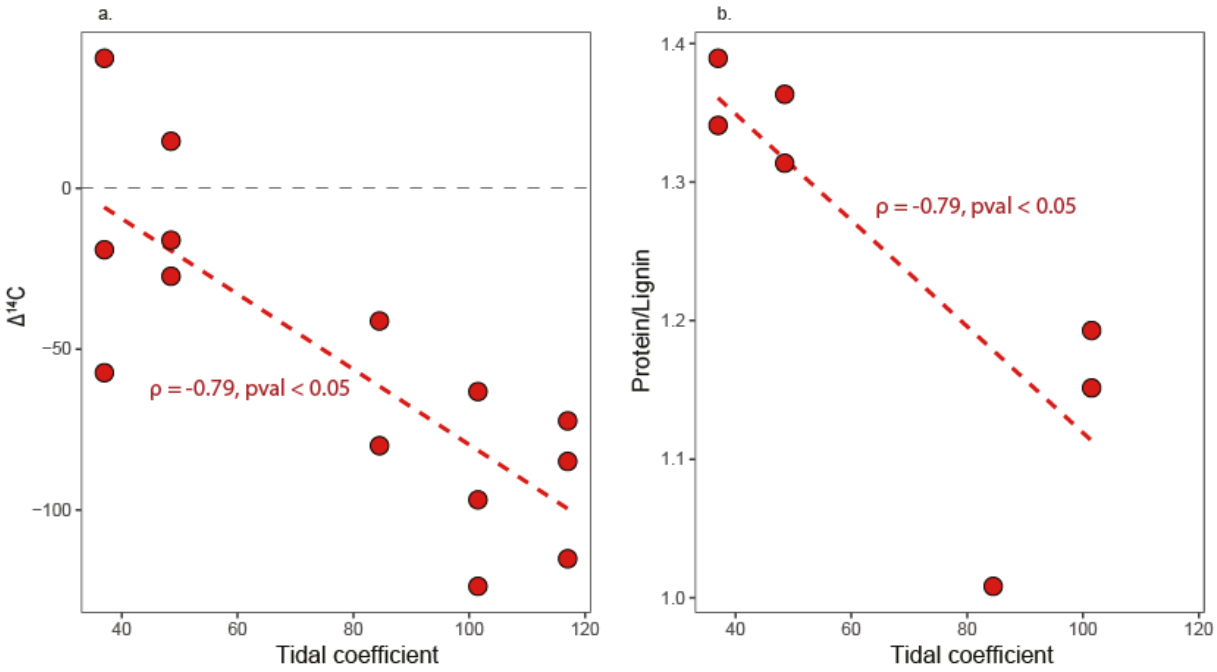

Figure 8:

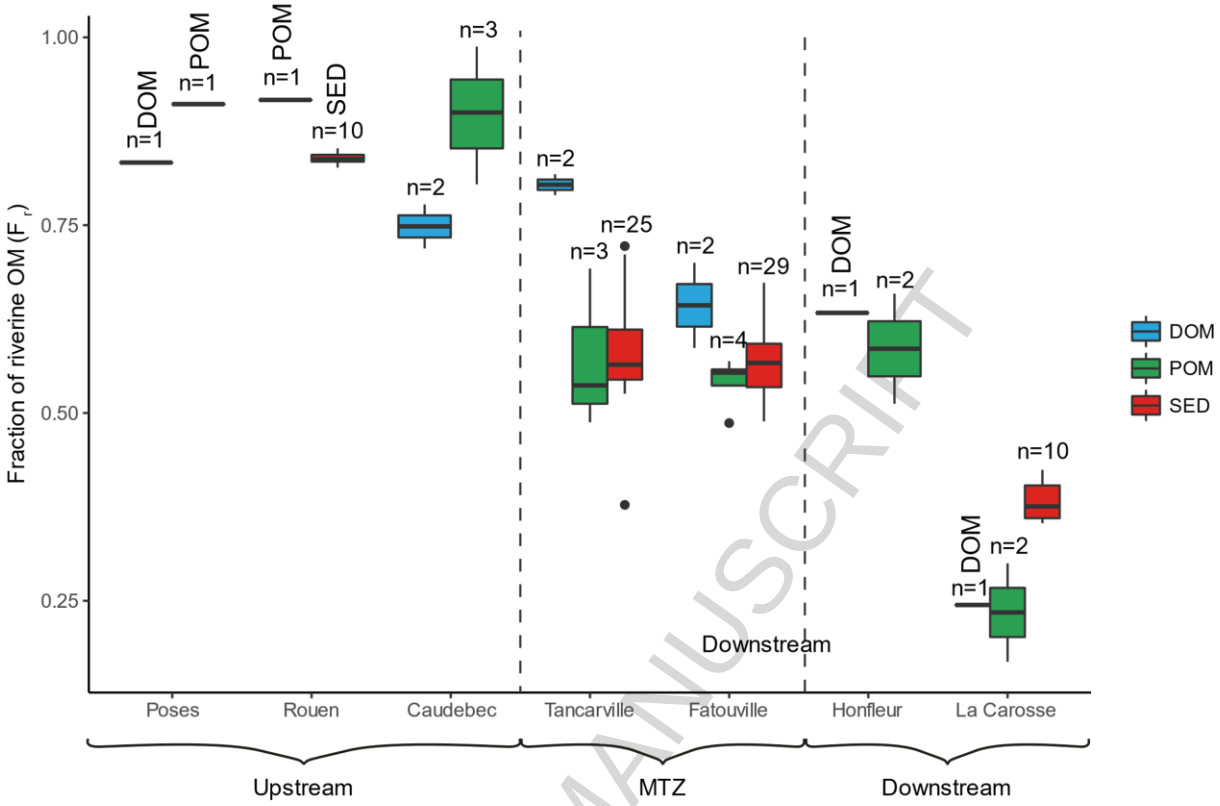

Figure 9:

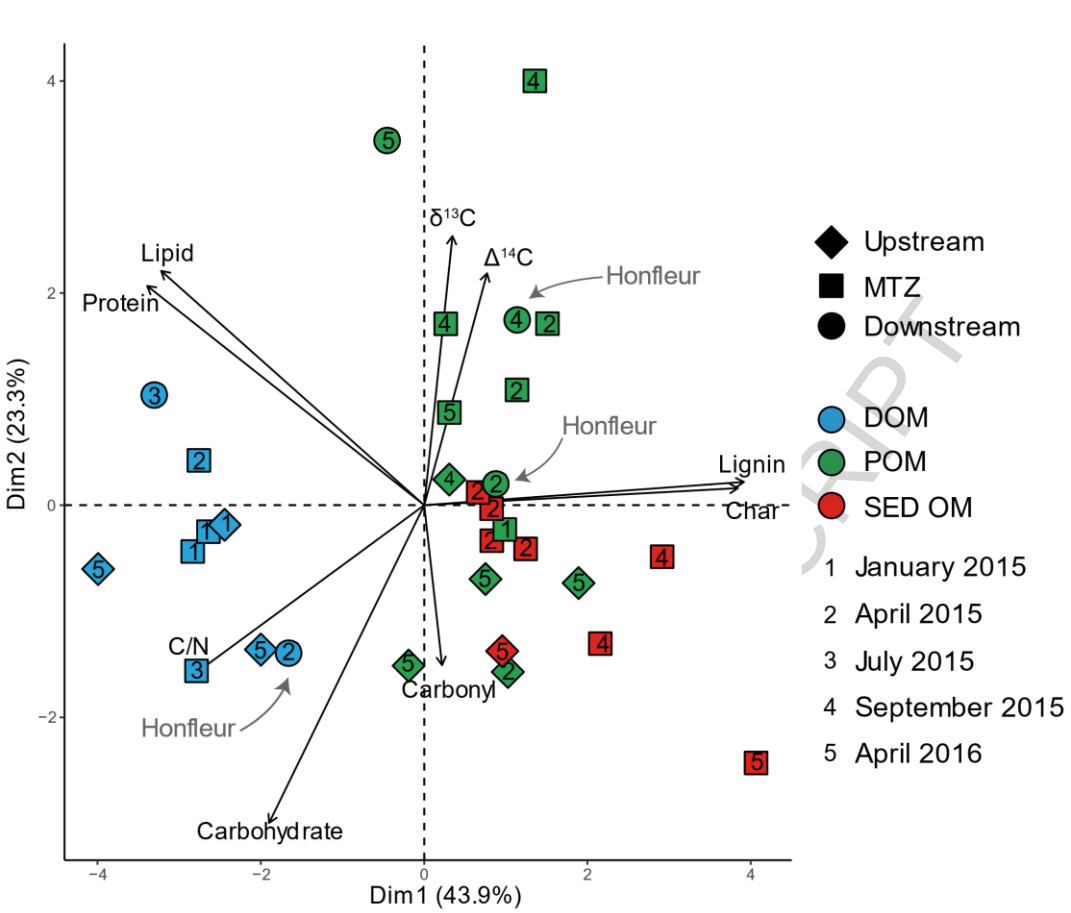

Table 1: DOC recovery after concentration and desalting of water samples by RO/ED. *DOC is not available for this sample and was set to the concentration observed in the upstream part of the estuary (Rouen).

Sample Location	Campaign	Initial volume (L)	Final volume (L)	Initial DOC (mg/L)	Final DOC (mg/L)	Yield (%)	Salinity
Tancarville	January 2015	102	6.8	2.5	32.5	87	0.4
Caudebec	April 2015	106	5.9	3.3	42.5	73	0.3
Tancarville		41.5	3.2	1.7	16.5	72	0.6
Fatouville		102	6.3	1.8	15.1	51	17.7
Honfleur		101.5	4.8	2.2	20.8	44	19.9
Fatouville	July 2015	102.3	5.3	1.7	23.3	69	2.7
La Carosse		102	3.5	1.3	9.5	26	32.3
Poses	April 2016	103.5	3.3	2.5*	37	47	0
Caudebec		105.8	6	2.1	21.4	58	0.3

Highlights

- Sources and fate of Seine Estuary organic matter (OM) investigated
- Dissolved, particulate and sediment OM mainly of recent aquatic origin
- River-dominated (recent DOM/POM) *vs.* marine-dominated (old DOM/recent POM) zones
- ^{13}C NMR-based Protein/Lignin ratio promising proxy to discriminate OM sources
- OM quality mainly related to the compartment and secondly to the sampling zone